Mass Transfer from a Solid Sphere to Water in Highly Turbulent Flow

L. R. STEELE and C. J. GEANKOPLIS

The Ohio State University, Columbus, Ohio

Mass transfer coefficients from ½-in. spheres of benzoic and cinnamic acids and 2-napthol to water were measured in the high Reynolds number region of 600 to 140,000. Previous data for liquids extended only to a Reynolds number of 11,000. Three separate and approximately parallel lines of J_D vs. Reynolds number were found for the different solutes, and the shape of the curves was found to be similar to the total-drag-coefficient correlation for spheres.

Experiments with benzoic acid and 2-napthol showed an effect of driving force and hence flux on the J_D values. Mass transfer did occur in saturated solutions having zero driving force. When one subtracted the amount of mass transfer at zero driving force from the values at other driving forces, the corrected J_D values at different driving forces were the same for a given solute. Possible explanations may be the effect of extreme turbulence on crystallization or physical attrition.

The transfer of mass from single spheres to a flowing liquid at low velocity or low Reynolds number has been extensively studied by a number of investigators (*4, 5, 7, 8*), and a correlation was presented by Garner and Suckling (*5*). However few data are available above a Reynolds number of 1,000 and none above 11,000. The effect of varying the Schmidt number for a given solute and for different solutes and the effect of mass flux on the mass transfer coefficients have not been studied in the very turbulent region and only sparingly in the low Reynolds number region.

In the present experimental work, ½-in. spheres of benzoic and cinnamic acids and 2-naphthol were used, and mass transfer coefficients were measured at a Reynolds number between 600 and 140,000. The effects of mass flux and Schmidt number were also investigated.

LITERATURE REVIEW AND THEORY

In mass transfer from dissolving solids to flowing liquids the driving force is assumed to be the saturation solubility adjacent to the solid minus the bulk-stream concentration. In most previous investigations (*4, 5, 7, 8*) the bulk-stream concentration was kept constant at approximately zero. The mass transfer flux and mass transfer coefficient are related by

$$N_A = K_L(C_s - C'_L) \qquad (1)$$

To reduce the mass flux at a given temperature and Reynolds number C_L can be increased from the normal zero value.

The dimensionless number of Chilton and Colburn (*2*) is defined as

$$J_D = \frac{K_L}{V}\left(\frac{\mu}{\rho D_L}\right)^{2/3} \qquad (2)$$

The J_D factor has been correlated against the Reynolds number $D_p V\rho/\mu$ for spheres.

Linton and Sherwood (*7*) determined J_D values for individual benzoic acid spheres for a Reynolds number range of 1,500 to 11,000. The spheres were mounted in the center of the pipe and supported by a metal wire normal to the flow. Data were also obtained for transverse cylinders with cinnamic and benzoic acids, with the J_D for benzoic acid being approximately 20% higher than for cinnamic acid.

McCune and Wilhelm (*8*) used a 2-naphthol pellet which was resting on a wire screen, up through which the liquid flowed. Data were obtained for a Reynolds number range of 30 to 500, in which the pellet was essentially immobile on the screen.

Garner and Suckling (*5*) determined J_D values for single spheres of adipic and benzoic acids for a Reynolds number range of 30 to 700. The spheres were supported by an axial rod on the downstream side. They correlated their data and those of Garner and Grafton (*4*) and found that for Reynolds numbers greater than 100 above the natural-convection region

$$J_D = (\text{constant})\, N_{Re}^{-0.5} \qquad (3)$$

Dryden, Strang, and Withrow (*3*) found that at Reynolds numbers below 10 in packed beds values of J_D for benzoic acid were greater than for 2-naphthol.

Goldstein (*6*) discussed the drag on a sphere and stated that spheres supported by a cross wire will disturb the flow continuity over the sphere surface and give a total drag up to double that when the sphere is held at the back by an axial spindle. He gives a plot of total drag vs. Reynolds number values up to 4,000,000. At low Reynolds numbers the drag coefficient decreases with increasing Reynolds numbers and levels off in the Reynolds number region of 5,000 to 250,000. Then the drag coefficient suddenly drops over 50% and then increases. Binder (*1*) discusses the changes in the flow patterns and wakes which cause these unusual changes in the drag coefficient. It would be expected that these phenomena should cause somewhat similar changes in the J_D vs. Reynolds number plot.

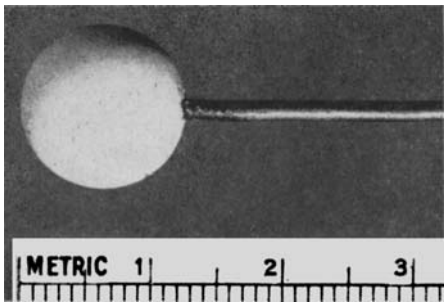

Fig. 1. Cinnamic acid sphere after a run.

EXPERIMENTAL METHODS AND RESULTS

Materials and Spheres

The three different types of solute crystals used were benzoic acid, trans-cinnamic acid, and 2-naphthol. Distilled water was used for all runs. The ½-in. spheres were made by casting in plaster-of-Paris molds. An 0.064-in. brass wire 1½-in. long was cast into the sphere. This wire was the spindle mount holding the sphere axially from the rear. The wire was inserted for ¾ in. into a larger supporting rod.

The molded sphere was easily removed from the casting and was washed with water and dried in a desiccator before being weighed. After mass transfer the sphere was again dried and weighed. The diameter was measured in four directions before and after a run, and the average was used. The maximum change in diameter during a run was less than 0.8%. Figure 1 shows a typical cinnamic acid sphere after a mass transfer run.

Apparatus

In the process flow (Figure 2) the distilled water was drawn from storage and pumped

TABLE 1. EXPERIMENTAL SOLUBILITY DATA IN WATER

Solute	Temperature, °C.	C_s', g./liter
Cinnamic acid	25.0	0.491
Cinnamic acid	34.3	0.700
Cinnamic acid	21.5	0.460
Cinnamic-acid spheres	25.0	0.495
Benzoic acid	25.0	3.38
Benzoic acid	34.3	4.85
Benzoic acid	21.5	3.06
Benzoic-acid spheres	25.0	3.40
2-Naphthol	25.0	0.725
2-Naphthol spheres	25.0	0.740

L. R. Steele is with Argonne National Laboratories, Lemont, Illinois.

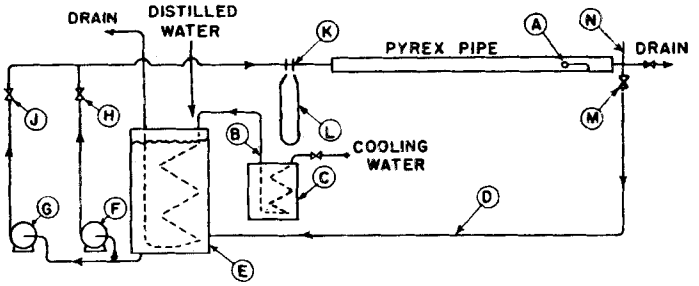

Fig. 2. Process-flow diagram: A = cast sphere, B = cooling-water line, C = ice bath, D = return line, E = stainless steel drum, F = small pump, G = large pump, H = globe valve, J = globe valve, K = orifice, L = manometer, M = recycle valve, N = thermometer.

through an orifice to the 1½-in. I.D. Pyrex test section. The test sphere was mounted 15 in. from the downstream end of the pipe, which was 10 ft. long. The water was recirculated and the temperature controlled. Depending on the type of solute used, runs lasted for as long as 4 to 60 min.

Solubility Determinations

The solubilities of the three solutes were experimentally determined (Table 1). An excess of crystals was placed in a glass-stoppered Erlenmeyer flask and covered with a rubber stall. The flask was totally immersed in a constant-temperature bath and agitated for one day by a magnetic stirrer. The clear solution was pipetted and analyzed with a Beckman DK-2 spectrophotometer. The absorption peak was 270 mμ for cinnamic acid, 226 for benzoic, and 225 for 2-naphthol. Knowns were run and results interpolated. Identical results were also obtained with cast spheres instead of crystals.

Data from Table 1 are plotted (Figure 3) and show that the value for 2-naphthol checks those of McCune and Wilhelm (*8*). The data for benzoic acid check those from Seidell (*9, 10*). The data for cinnamic acid from Seidell scatter widely. The values used in calculations of J_D are those taken from the solid lines in the plot.

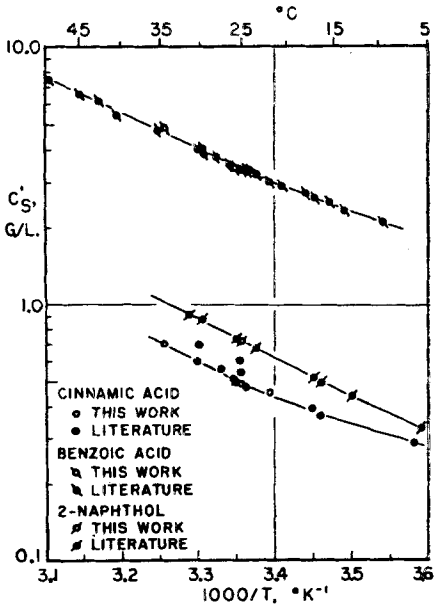

Fig. 3. Solubilities.

Diffusivities Used

The available diffusivity data are plotted as Schmidt numbers in Figure 4. Linton and Sherwood (*7*) give experimental data for benzoic and cinnamic acids from 10° to 25°C. For the range of 25° to 35°C. the Wilke equation (*11*) was used for extrapolation of the temperature effect. For 2-naphthol the experimental data (*8*) for 15° to 21°C. were plotted, and a line was drawn through the middle of these three points parallel to the other two lines. In developing his equation Wilke (*11*) shows a maximum deviation of about 25% and an average of 6%. Values of the three solutes predicted with the Wilke equation had a maximum deviation of less than 25%. The values used to calculate J_D are those taken from the lines in Figure 4.

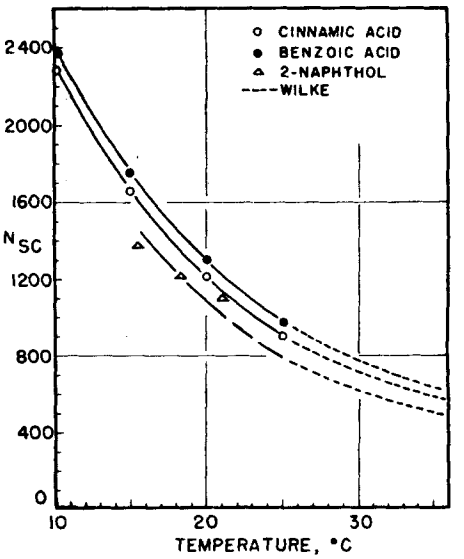

Fig. 4. Schmidt number vs. temperature.

Table 2. Mass Transfer Data (Axial Mounting of Sphere)**

Solute	D_p, cm.	V', cm./sec.	Temperature, °C.	C_s', g./liter	C_L', g./liter	$K_L/V \times 10^5$	N_{Sc}	$J_D \times 10^3$	N_{Re}
Cinn.	1.270	640	25.3	0.495	0	5.76	885	5.37	102,000
Cinn.	1.275	106	24.5	0.490	0	7.21	925	6.85	16,900
Benz.	1.267	103	25.0	3.40	0	8.53	970	8.37	16,350
2-Naph.	1.265	141	25.0	0.725	0	4.55	785	3.87	22,400
Cinn.	1.275	308	34.9	0.713	0	9.29	573	6.42	60,400
2-Naph.	1.277	527	25.3	0.725	0	3.94	773	3.31	86,000
2-Naph.	1.270	218	21.1	0.630	0	3.25	1003	3.27	31,800
Benz.†	1.270	249	25.7	3.45	3.01	15.60	940	14.92	40,200
Benz.‡	1.260	128	25.0	3.40	3.40	1.060‡	970	1.038‡	20,200
Benz.†	1.250	124	25.0	3.40	1.70	9.13	970	8.93	19,400
2-Naph.‡	1.274	133	25.0	0.725	0.725	0.213‡	785	0.184‡	21,200
2-Naph.†	1.257	150	25.3	0.725	0.330	4.93	744	4.15	23,700
Cinn.*	1.277	58.6	24.8	0.495	0	10.27	906	9.45	9,490
2-Naph.*	1.273	58.6	24.9	0.725	0	7.50	790	6.32	9,410
Benz.*	1.273	58.6	25.0	3.40	0	10.84	970	10.45	9,320

*Cross wire instead of axial spindle.
**Tabular material has been deposited as document 5877 with the American Documentation Institute, Photoduplication Service, Library of Congress, Washington 25, D. C., and may be obtained for $1.25 for photoprints or $1.25 for 35-mm. microfilm.
†Reduced flux.
‡Saturated solution; calculated as if $C_L = 0$.

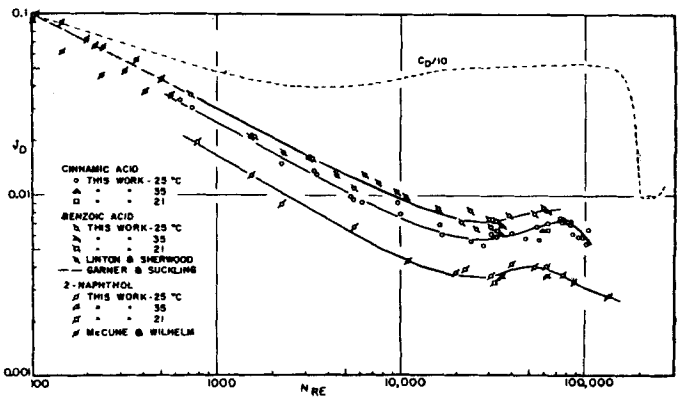

Fig. 5. J_D vs. Reynolds number.

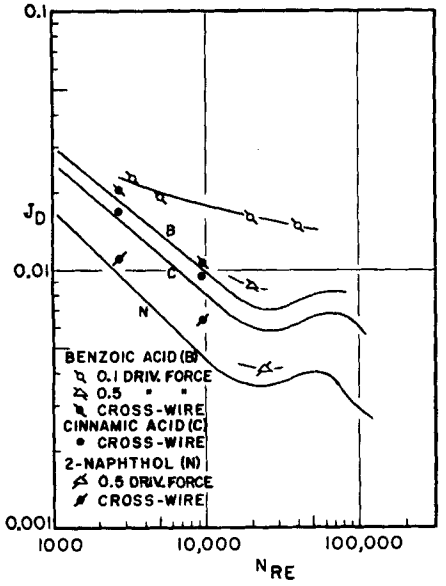

Fig. 6. Effect of flux and type of sphere mounting on J_D.

Calculation of J_D

The experimental data were used to calculate J_D as follows. From weight loss, duration of run, and average diameter, N_A was calculated. With the solubility data in Figure 3, Figure 4, velocity data, and Equations (1) and (2), J_D was then calculated. The average velocity in the annular free space between the sphere and the pipe wall was used. The data are given in Table 2.

DISCUSSION

Correlation of J_D vs. Reynolds Number

The mass transfer data are plotted in Figure 5. There are three distinct lines with the benzoic-acid line being about 25% above the cinnamic and the cinnamic being about 55% above the 2-naphthol line. Linton and Sherwood (7) at Reynolds numbers below 11,000 found the J_D for benzoic acid to be about 20% above the values for cinnamic acid for cross cylinders. Dryden and coworkers (3) also found J_D values for benzoic acid to be greater than those for 2-naphthol.

Data of other investigators plotted in Figure 5 were corrected by the use of the average velocity in the annular-free space. The Garner and Suckling line (5) for benzoic acid when extended past a Reynolds number of 700 checks the present benzoic acid correlation. The data of Linton and Sherwood (7) for benzoic acid also check the present work. The 2-naphthol data of McCune and Wilhelm (8) at low Reynolds numbers appear to be somewhat higher than the extrapolation of the 2-naphthol line through the present work; this may be due to their use of a screen before the pellet. The leveling off of the J_D values at high Reynolds numbers and then the drop are similar to the total drag correlations of Goldstein (6).

At all Reynolds numbers the benzoic acid line is about 80% above the 2-naphthol line. Hence this spread cannot be due to errors in the diffusivity but must be due to other causes. Visual inspection of the spheres showed them to be quite smooth before mass transfer and to have only a slight roughness on the surface after the runs. Several experiments were performed with the same sphere used for several different runs, and no trends were noticed. Also in one case the sphere was artificially roughened before the run, and no effect was apparent.

A detailed analysis of the errors in the determination of J_D was made for such errors as those which occurred in weighing, orifice calibration, temperature and diameter measurement, etc. The maximum known error was calculated to be $\pm 10\%$. In Figure 5 the maximum deviation of the data from each average line is 15% for the cinnamic acid line, and the average deviation is $\pm 5\%$. These small errors cannot account for the three different lines found. In the runs for a given solute the temperature was varied from 21° to 35°C., which changed the Schmidt number twofold. All these data fall near the proper line, which confirms the two-thirds exponent for a given solute.

Effect of Type of Sphere Mounting

In Figure 6 several runs are plotted in which the sphere was mounted by a cross wire instead of an axial spindle at the rear. These data give J_D values about 10 to 30% higher. The data of Linton and Sherwood (7) in Figure 5 were also obtained with a cross-wire mount and those of McCune and Wilhelm (8) with a screen which might be termed a multiple cross-wire mount.

Flux Effects

It was speculated that the mass flow or flux might interact, or have a coupling effect on the boundary layer, or change the bulk properties which would change J_D. Benzoic acid, which has the largest solubility, would have the greatest flux, since the driving force is $(C_s - C_L)$, where C_L is zero. To check this the C_L was made greater than zero in several runs, so that the driving force was reduced to about 10% of the original maximum for benzoic acid. This should have reduced the flux to a value close to that of 2-naphthol. The data in Figure 6 show

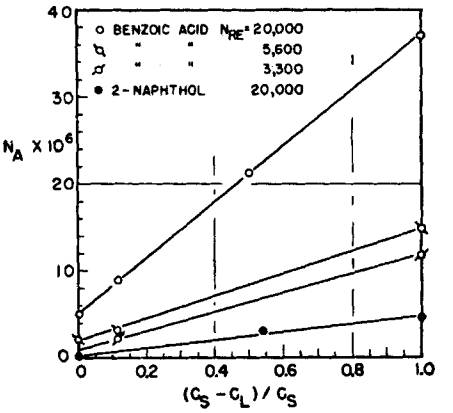

Fig. 7. Effect of driving force on flux.

that the J_D values are much greater at low flux values then at maximum flux and that the low flux benzoic acid and high flux 2-naphthol lines are not the same. Also at low Reynolds numbers the effect of flux decreases markedly.

Several runs were also made in a saturated solution with the sphere which should give a zero driving force. Some mass transfer did occur in these runs, and the flux data are shown in Figure 7. Subtracting this zero driving-force flux value from the others in Figure 7 one can calculate a corrected N_A and J_D for each driving force (Table 3). These corrected values of J_D are approximately constant and independent of driving force for benzoic acid and 2-naphthol. The corrected values for benzoic acid are not equal to those for 2-naphthol; hence other reasons must be sought for the differences in the J_D values of the three solutes.

Another way used to attempt to correct the J_D for driving-force effects for benzoic acid was to assume a pseudo solubility at other temperatures. By trial and error it was found that at an assumed temperature of 29°C. the J_D values for benzoic acid check for different driving forces. An estimate of the temperature rise at the sphere surface due to friction drag showed an insignificant temperature rise. Hence the significance of this 29°C. temperature is not apparent. For 2-naphthol this pseudotemperature was found to be about 26°C.

An explanation of this mass transfer at saturation or zero driving force could be derived from the concept of equilibrium at saturation and attrition. At

TABLE 3. EFFECT OF ZERO DRIVING-FORCE FLUX AT N_{Re} = 20,000

Solute	Percentage of maximum driving force	$J_D \times 10^3$	$N_A \times 10^6$	J_D corrected $\times 10^3$
Benzoic	100	7.06	37.2	6.08
Benzoic	50	8.93	21.5	6.80
Benzoic	11.5	16.05	9.02	6.84
Benzoic	0	——	5.16	
2-Naphthol	100	3.77	4.54	3.58
2-Naphthol	54	4.15	3.27	3.85
2-Naphthol	0	——	0.23	

high turbulence a steady state dynamic equilibrium is present in the saturated solution. The mass flux from the sphere (dissolution) is equal to the mass flux to the sphere (crystallization). The material going to the sphere must crystallize on the surface by the growth of existing crystals and possibly by the formation of new crystals. Some crystals may grow larger than others; this makes the surface more irregular and less densely packed than before. These new, fine crystals could have difficulty in adhering to the surface in the highly turbulent stream. Hence these enlarged, existing crystals or the new crystals could easily be broken off and carried away in the main stream.

This mass transfer at zero driving force could also be due to physical attrition, where eddies tear off or wear away minute particles of the cast solid other than those actually dissolved by true mass transfer. If mass transfer due to this type of attrition is present, it should be an additive effect along with the true dissolution mass transfer. However, as discussed previously, this correction gives constant J_D values for a given solute (Table 3) but does not give the same values for all solutes. Hence attrition alone is probably not causing these differences. It should be noted that the mass transfer at zero driving force for benzoic acid increases with increasing Reynolds numbers (Figure 7). Preliminary hardness tests made on the cast spheres indicated that 2-naphthol was the hardest material and benzoic acid the softest.

Further studies should be made in mass transfer from dissolving solids in turbulent fluids on the role of physical properties of the solute such as hardness, crystalline structure, and ability to crystallize.

NOTATION

C_D = total drag coefficient for spheres.
C_s = concentration of solute in saturated solution, g./cc.
C_s' = concentration of solute in saturated solution, g./liter.
C_L' = concentration of solute in solution, g./liter.
C_L = concentration of solute in solution, g./cc.
D_L = molecular diffusivity, sq. cm./sec.
D_p = diameter of sphere, cm.
J_D = dimensionless number for mass transfer.
K_L = mass transfer coefficient, g./(sq. cm.)(sec.), g./cc.
N_A = flux, g./(sq. cm.)(sec.)
N_{Re} = Reynolds number = $D_pV\rho/\mu$
N_{Sc} = Schmidt number = $\mu/\rho D_L$
V' = average velocity in pipe, cm./sec.
V = average velocity in annular area between pipe and sphere, cm./sec.
μ = viscosity, g./(sec.)(cm.)
ρ = density, g./cc.

LITERATURE CITED

1. Binder, R. C., "Advanced Fluid Dynamics and Fluid Machinery," p. 116, Prentice Hall, New York (1951).
2. Chilton, T. H., and A. P. Colburn, *Ind. Eng. Chem.*, **26**, 1183 (1934).
3. Dryden, C. E., D. A. Strang, and A. E. Withrow, *Chem. Eng. Progr.*, **49**, 191 (1953).
4. Garner, F. H., and R. W. Grafton, *Proc. Roy. Soc. (London)*, **A224**, 64 (1954).
5. Garner, F. H., and R. D. Suckling, *A.I.Ch.E. Journal*, **4**, 114 (1958).
6. Goldstein, Sydney, "Modern Measurements in Fluid Mechanics," p. 16, 491, Clarenden Press, Oxford (1938).
7. Linton, W. H., and T. K. Sherwood, *Chem. Eng. Progr.*, **46**, 258 (1950).
8. McCune, L. K., and R. H. Wilhelm, *Ind. Eng. Chem.*, **41**, 1124 (1949).
9. Seidell, Atherton, "Solubilities of Organic Compounds," 3 ed., Vol. II, D. Van Nostrand, New York (1941).
10. ———, and W. F. Linke, "Solubilities of Inorganic and Organic Compounds," Supplement to 3 ed., D. Van Nostrand, New York (1952).
11. Wilke, C. R., and Pin Chang, *A.I.Ch.E. Journal*, **1**, 264 (1955).

Manuscript received August 27, 1958; revision received November 6, 1958; paper accepted November 6, 1958.

Turbulent Flow of Pseudoplastic Polymer Solutions in Straight Cylindrical Tubes

ROBERT G. SHAVER and EDWARD W. MERRILL

Massachusetts Institute of Technology, Cambridge, Massachusetts

Experimental studies are described concerning the fluid dynamics, particularly in the turbulent region, of dilute solutions of free-draining, nonassociating, linear polymers; sodium carboxymethylcellulose, ammonium alginate, polyisobutylene, and carboxypolymethylene, all of which are pseudoplastic. These solutions were run in laminar, transition, and turbulent flow in a pipeline flow apparatus designed to permit measurement of dynamic pressure drop and impact pressure by radial traverse.

Photographic studies with dye injection used at the tube wall and at the tube center showed that turbulent flow of these pseudoplastic fluids has the following characteristics compared to Newtonian fluids: poor over-all radial mixing, thicker nonturbulent layer at the wall, and decreased rate of formation of horseshoe vortices at the wall.

A pseudoplastic fluid generally is defined as one which has a viscosity that decreases reversibly with increasing shear rate, which has no yield value, and which undergoes no time-dependent change in consistency. Dilute solutions of free-draining, essentially nonassociating polymers represent one class of pseudoplastic fluid, perhaps the most common. With one exception* the experimental studies described herein were concerned exclusively with this class of pseudoplastic fluid.

The shear-rate–shear-stress relationships of these polymer solutions can be correlated in general over a rather broad range of shear rates by the power-law model $\tau = b(du/dy)^s$ (*4, 8, 9, 10*).

Since the shear stress in a fluid flowing steadily in a straight cylindrical tube varies linearly from zero at the axis to a maximum $\tau_w = (\Delta P/L)\cdot(R/2)$ at the wall, the flow equations for pseudoplastics in laminar flow can be derived by assuming the power-law rheology (*3, 8*). The resultant expressions are friction factor:

$$f = [16b/(D^sV^{2-s}\rho)] \cdot [2(3 + 1/s)]^s/8 \qquad (1)$$

Robert G. Shaver is with the Dewey and Almy Chemical Company, Cambridge, Massachusetts.

*The exception is polyvinyl alcohol (Elvanol), which shows a strong tendency to associate by hydrogen bonding in dilute solution. The associating tendency in the Elvanol solution studies was so great that opalescence was noted, suggesting micelle formation. The results are irrelevant, since the solution behaved as a Newtonian fluid.